

## Extracting the number of quantum dots in a microenvironment from ensemble fluorescence intensity fluctuations

Inhee Chung, James B. Witkoskie, John P. Zimmer, Jianshu Cao, and Mounqi G. Bawendi

*Department of Chemistry and Center for Materials Science and Engineering, Massachusetts Institute of Technology, 77 Massachusetts Avenue, Cambridge, Massachusetts 02139, USA*

(Revised manuscript received 19 April 2006; revised manuscript received 16 October 2006; published 8 January 2007)

We estimate the number of CdSe quantum dots (QDs) in a microenvironment by analyzing the intensity fluctuation of the fluorescence time trace from a collection of QDs in the fluorescence intensity steady-state regime. The steady state is chosen because the aged blinking dynamics of single QDs leads to a higher probability for observing large on and off waiting times relative to the typical time bins chosen to generate fluorescence time traces. In the steady state, the relative standard deviation of the fluorescence intensity from a collection of QDs is bin-size independent, which enables a simple estimation of the absolute number of QDs under observation. This is not possible for most conventional chromophores, whose triplet blinking dynamics are much faster than a typical bin size, or for QDs undergoing blinking dynamics that are fast compared to the bin size, as occurs prior to the steady state. The estimated number of QDs incorporated into a single silica microsphere as determined by our method agrees well with the number obtained using conventional absorption measurements on an ensemble of microspheres.

DOI: [10.1103/PhysRevB.75.045311](https://doi.org/10.1103/PhysRevB.75.045311)

PACS number(s): 78.55.-m, 05.40.-a, 78.67.Bf, 82.37.-j

The number of photons randomly emitted from  $N$  conventional chromophores during a typical time bin  $t_b$ , used to generate a fluorescence time trace, usually approximately follows Poisson statistics, with a standard deviation (SD) that scales as  $(Nt_b)^{0.5}$ . On the other hand, as we show in this paper, the SD of the number of emitted photons during a similar time bin  $t_b$  from  $N$  CdSe semiconductor quantum dots (QDs) whose ensemble fluorescence intensity has reached the steady state<sup>1,2</sup> exhibits a scaling of  $N^{0.5}t_b$ . Conventional chromophores often have short-lived dark triplet states, which results in rapid blinking compared to  $t_b$ , so that the fluctuations in the number of photons mainly stem from photon emission statistics, resulting in a  $(Nt_b)^{0.5}$  scaling for the SD of the photon number. There have been observations of conventional chromophores exhibiting power-law blinking in the long-time limit.<sup>3</sup> Their photodynamics are often complicated by their intrinsic triplet blinking, which is superimposed on the long-time scale blinking dynamics arising from their interactions with the surrounding environment, as well as fast photobleaching. In this work therefore we confine our discussion of conventional chromophores to those that exclusively display triplet blinking dynamics. For QDs in the steady state,<sup>1,2</sup> there is a reasonable probability of observing both “on” and “off” waiting times that are long with respect to  $t_b$ , so that the blinking process largely determines the fluctuations in the number of emitted photons, resulting in the approximate  $N^{0.5}t_b$  scaling of the SD for  $t_b$  smaller than the average lengths of on and off waiting times.

A steady state exists in the long-time limit of fluorescence time traces from a collection of QDs (CQD) when the aging process for the on and off waiting times reaches maturity.<sup>1,2</sup> In fact, the steady state can be understood by correlating the single QD fluorescence blinking statistics to the fluorescence time trace of the CQD. For the single QD fluorescence blinking that has been the subject of many studies,<sup>1,2,4-18</sup> the on and off events appear to be uncorrelated and the corresponding waiting times follow approximate power-law statistics

bounded by lower and upper cutoffs.<sup>1,2</sup> The particular values of the cutoffs are related to the characteristics of the QD and its surrounding environment. Similar forms of power-law statistics have been observed for CdSe QDs dispersed in liquid, deposited on glass or metal, or embedded in polymer.<sup>4,7-9,18-21</sup> It is not usually practical to determine cut-off values through single QD fluorescence measurements but they can be simply estimated from the ensemble measurement.<sup>1,2</sup> The upper cutoffs can be estimated from the long-time limit of the fluorescence time trace of a CQD. The nonuniversal behavior observed in the early fluorescence time trace of a CQD can be explained through the ratio of the lower cutoffs and the initial quantum yield.<sup>2</sup> The exact functional forms and values for the lower cutoffs have not yet been measured experimentally. Instead, our previous work suggests an approximate methodology for extracting the ratio between the lower cutoffs by assuming arbitrary functional forms and showing that the ratio is not significantly affected by the functional form.<sup>2</sup> Our previous work also shows that the fluorescence time trace of a CQD is composed of four sequential time windows which consist of (i) a nonuniversal short-time dynamic region, (ii) a transient equilibrium state (this is observed only when the on- and off-time power-law exponents are approximately equal to each other), (iii) a power-law decaying region, and (iv) a long-time limit steady state.<sup>1,2</sup> The steady state is reached when a CQD is excited under continuous excitation for a time period longer than the off-time upper cutoff.

There have been other studies that connect the fluorescence intensity fluctuations of a CQD to the power-law blinking statistics of single QDs. Pelton *et al.* found an approximate  $1/f$  noise in the power spectrum of the fluorescence intensities from both a CQD and single QDs, and explained the form of the noise in terms of the power-law statistics of single QDs.<sup>20</sup> As previous experiments suggest,<sup>1,2</sup> cutoffs must exist in the  $1/f$  functional form at low frequencies, implying the emergence of a steady state in

the long-time limit of the fluorescence time trace of a CQD. In addition, a characteristic power-law process similar to the blinking statistics of a single QD was also recently demonstrated in the noise analysis of the current response performed by conductivity measurements on arrays of CdSe QDs.<sup>21</sup>

In this paper, we make use of our previously published methodology<sup>1,2</sup> that extracts single QD blinking statistics from a fluorescence time trace of  $N$  QDs to show how those extracted statistical parameters can be used to easily estimate the number of QDs under observation. We first construct a general theoretical formula for the relative standard deviation (RSD) of the fluorescence intensity from  $N$  arbitrary chromophores acquired during a time bin of width  $t_b$ . The RSD is simply the inverse square of the signal-to-noise ratio (SNR),  $\text{RSD}=(1/\text{SNR})^{1/2}$ . For simplicity in this paper we confine the value of  $t_b$  to range from  $10^{-2}$  to 1 sec, a typical time bin range for sequential time imaging experiments. We then apply this general formula to the RSD of the fluorescence intensity from a CQD in its steady state, demonstrating that the RSD is nearly independent of  $t_b$  within an appropriate range. This is then validated by simulation and experiments. The experiments further imply that the values for lower cutoffs are much smaller than typical  $t_b$ 's. Finally, we show that the  $t_b$ -independent RSD for a CQD in the steady state provides a simple methodology to estimate the absolute number of QDs under observation. Although our proposed method for estimating the number of QDs under observation is approximate, the advantage of this method is its widespread applicability. Other methods for extracting the number of QDs from an ensemble measurement can be more difficult to implement, for example optical absorption<sup>22</sup> or combining atomic force microscopy (AFM) and fluorescence microscopy.<sup>23</sup> In this manuscript, we use our proposed methodology to extract the number of QDs that are embedded in a submicron-sized silica microsphere<sup>24</sup> and compare this with the value obtained from a conventional absorption experiment.<sup>22</sup> Ultimately our methodology rests on the identification of the steady state as the appropriate time window for estimating the number of QDs.

We first summarize our previous model that relates single QD blinking statistics to the average fluorescence time trace of a CQD.<sup>1,2</sup> The mathematical form of the average time trace corresponds to the time-dependent probability function  $f_{on}(t)$  for a single QD to be capable of emission (a QD that is "on"). The function  $f_{on}(t)$  can be constructed from the probability distribution functions  $p_{on(off)}(t)$  for the on (off) waiting times, respectively. The functions  $p_{on(off)}(t)$  are bounded power-law probability density functions with power-law exponents  $\mu_{on(off)}$ , which we assigned as 0.5 according to experiments, and the bounds are exponential cutoffs with characteristic times  $t_{on(off)}^{min}$  and  $t_{on(off)}^{max}$ . When time  $t$  approaches  $t_{on}^{max}$ , a transient equilibrium state can be formed, which is followed by a power-law decay when  $t > t_{on}^{max}$ , and finally by a steady state when  $t > t_{off}^{max}$ . The function  $f_{on}(t)$  is approximately constant with values  $f_{on}^{te}$  and  $f_{on}^{ss}$  during the transient equilibrium (*te*) and steady states (*ss*), respectively.

We then theoretically describe the general form of the RSD for arbitrary chromophores where the total number of

chromophores in the sample is fixed at  $N_T$ . The mean and standard deviation for the number of photons  $I_{Tphoton}$  emitted from  $N_T$  chromophores during a time bin  $t_b$  can be formulated as follows (see the Appendix):

$$\langle I_{Tphoton} \rangle = N_T \lambda \left\langle \int_{t'}^{t'+t_b} dt 1_{on}(t) \right\rangle, \quad (1)$$

$$\langle \delta^2 I_{Tphoton} \rangle = N_T \left[ \lambda^2 \left\langle \delta^2 \left( \int_{t'}^{t'+t_b} dt 1_{on}(t) \right) \right\rangle + \lambda \left\langle \int_{t'}^{t'+t_b} dt 1_{on}(t) \right\rangle \right], \quad (2)$$

where  $t'$  is an arbitrary starting point for a time interval of length of  $t_b$ , and  $1_{on}$  is an indicator function that is equal to 1 if a chromophore is on and 0 if it is off.  $\lambda$  is a Poisson parameter, representing the mean number of emitted photons per unit time from a single chromophore at a given excitation intensity. The RSD for  $I_{Tphoton}$  is by definition the ratio  $\sqrt{\langle \delta I_{Tphoton}^2 \rangle} / \langle I_{Tphoton} \rangle$ . After integration and averaging, the full expressions for Eqs. (1) and (2) are complicated, and hence we use approximations in order to obtain simplified forms for the RSD for the case of QDs in the steady state, and for conventional chromophores or QDs prior to the steady state, as described below.

An aged QD in the steady state is prone to blink slowly with respect to a typical value of  $t_b$ , and therefore the term  $\langle \delta^2 (\int_{t'}^{t'+t_b} dt 1_{on}(t)) \rangle$  in Eqs. (1) and (2) cannot be ignored. In addition, compared to the typical bin size  $t_b$ ,  $\lambda$  is typically a large number for a QD considering the high excitation flux and a radiative lifetime on the order of 20 ns.<sup>25</sup> As a result,  $\lambda^2 \langle \delta^2 (\int_{t'}^{t'+t_b} dt 1_{on}(t)) \rangle$  in Eq. (2) dominates over the second term  $\lambda \langle \int_{t'}^{t'+t_b} dt 1_{on}(t) \rangle$ . With the approximation that a QD is either on or off during one single bin in the steady state, the probability to find an on QD at an  $i$ th bin follows binomial statistics. Therefore the mean and standard deviation for the number of on QDs in a binned time trace during the steady-state regime are approximately

$$\left\langle \int_{t'}^{t'+t_b} dt 1_{on}(t) \right\rangle \approx p_{on} t_b, \quad (3)$$

$$\sqrt{\delta^2 \left( \int_{t'}^{t'+t_b} dt 1_{on}(t) \right)} \approx \sqrt{p_{on}(1-p_{on})} t_b, \quad (4)$$

where  $p_{on}$  is the average ratio of the number of on QDs per  $t_b$  in the steady state out of the total number of QDs  $N_T$ , and therefore  $p_{on}$  is equal to  $f_{on}^{ss}$ .<sup>1,2</sup> Using Eqs. (3) and (4), the ratio  $\sqrt{\langle \delta I_{Tphoton}^2 \rangle} / \langle I_{Tphoton} \rangle$  can be re-expressed as Eq. (5),

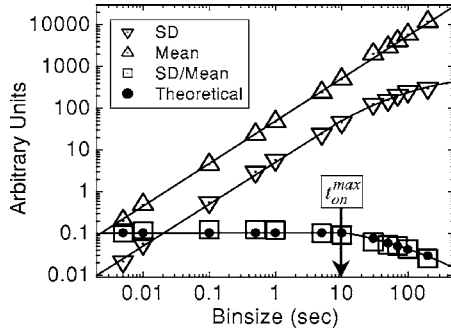


FIG. 1. We calculate the mean (upper triangle), standard deviation (lower triangle), and RSD (square) from the steady-state region of the intensity time traces of a CQD, created by Monte Carlo simulations with these conditions imposed: (i)  $N_T=500$ , (ii) on- and off-time power-law statistics with identical power-law exponents at  $\mu_{on}=\mu_{off}=0.5$ , (iii)  $t_{on}^{max}=10$  sec and  $t_{off}^{max}=10^3$  sec, (iv)  $t_{on}^{min}=t_{off}^{min}=10^{-4}$  sec, and (v)  $t_b=0.005, 0.01, 0.1, 0.5, 1, 5, 10, 25, 50, 75, 100,$  and  $200$  sec. The plot is on a log-log scale. The arrow indicates the  $t_{on}^{max}$  value. The black dots from  $0.005$  to  $5$  sec are calculated using Eq. (5) and those from  $10$  to  $200$  sec are obtained assuming a  $(Nt_b)^{0.5}$  scaling. The black lines simply connect consecutive points.

$$\frac{\sqrt{\langle \delta I_{T_{photon}}^2 \rangle}}{\langle I_{T_{photon}} \rangle} \cong \frac{\lambda t_b \sqrt{N_T p_{on} (1 - p_{on})}}{\lambda t_b N_T p_{on}} = \sqrt{\frac{1 - p_{on}}{p_{on}}} \frac{1}{\sqrt{N_T}} \left( \approx \frac{1}{\sqrt{N_S}} (p_{on} \ll 1) \right), \quad (5)$$

where  $N_S$  is a mean number of on QDs during  $t_b$  in the steady state ( $N_T p_{on} \equiv N_T f_{on}^{ss} = N_S$ ). Note that the scaling factor for the ratio in Eq. (5) is a function of only two parameters,  $N_T$  and  $p_{on}$ , both of which are directly related to the number of on QDs, and not to the number of emitted photons.  $p_{on}$  is generally experimentally observed to be as small as or smaller than  $0.1$ , where the value varies depending on the photo-physical characteristics of QDs and their surrounding environment.

The approximation that leads to Eq. (5) can only be applied with a time bin  $t_b$  that satisfies the condition  $t_{on(off)}^{min} < t_b < t_{on}^{max}$  so that  $t_b$  is generally smaller than the on and off waiting times exhibited in the steady state. The typical values of  $t_b$  chosen for experiments are usually in the range  $t_b < t_{on}^{max}$ , with the condition  $t_{on(off)}^{min} < t_b$  also satisfied, as is verified below. In Fig. 1, we use a Monte Carlo simulation to validate this  $t_b$ -independent scaling of the RSD for the emitted photons from a CQD in the steady state when the condition  $t_{on(off)}^{min} < t_b < t_{on}^{max}$  is met. The mean (upper triangle symbols in Fig. 1) and standard deviation (lower triangle symbols in Fig. 1) values calculated from simulated intensities for  $500$  ( $\equiv N_T$ ) QDs in the steady state show a linear increase as  $t_b$  varies from  $5 \times 10^{-3}$  to  $10^1$  sec. As a result, their ratio (square symbols in Fig. 1) (their RSD), does not change much with varying  $t_b$  while  $t_{on(off)}^{min} < t_b < t_{on}^{max}$ . Therefore when  $t_{on(off)}^{min} < t_b < t_{on}^{max}$  is met, Eq. (5) can be applied to calculate the number of QDs within the collection. As  $t_b$  approaches and exceeds  $t_{on}^{max}$  as indicated by the arrow in Fig.

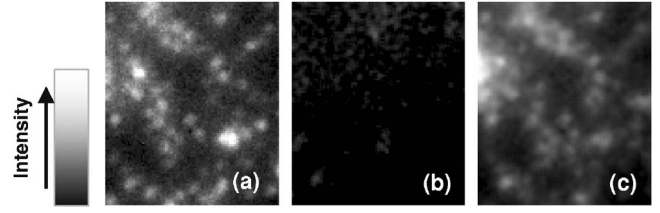


FIG. 2. A dilute solution of CdSe(ZnS) core-shell QDs dispersed in hexane (first absorption peak at  $605$  nm) was spin-coated onto a precleaned glass coverslip. The  $514$ -nm line from an Ar+ laser was used to continuously excite the sample at an excitation intensity of  $\sim 10$  kW/cm<sup>2</sup> at room temperature. (a) (b) A snapshot fluorescence image of single CdSe(ZnS) QDs spin-coated on a glass coverslip with  $t_b=0.2$  sec at  $t=8.2$  sec and  $5000$  sec, respectively. (c) Integrated fluorescence image from  $0$  to  $8000$  sec. The relative density of emissive QDs is similar in both (a) and (c). The intensity scheme is rescaled for each figure for best view and the relative intensities are indicated in gray scale as indicated.

1, the standard deviation begins to scale as  $\sqrt{t_b}$  as observed in Fig. 1. The theoretical RSD values (black dots in Fig. 1) when  $t_{on(off)}^{min} < t_b < t_{on}^{max}$  are calculated using Eq. (5) and are obtained by simply applying the scaling factor  $\sqrt{t_b}$  to the previous constant value when  $t_b > t_{on}^{max}$ . This transition can be explained by line-shape theory where  $t_{on(off)}^{min} < t_b < t_{on}^{max}$  is the static limit and  $t_{on}^{max} < t_b$  is the motional narrowing limit.

The motional narrowing limit corresponds to the photon emission statistics of conventional dye molecules. For those systems, triplet blinking, if applicable, occurs very fast compared to  $t_b$ , and as a result both  $\langle \delta^2 \int_{t'}^{t'+t_b} dt I_{on}(t) \rangle / \langle \int_{t'}^{t'+t_b} dt I_{on}(t) \rangle^2$  and  $1 / \langle \int_{t'}^{t'+t_b} dt I_{on}(t) \rangle$  scale with  $t_b^{-1}$  (due to the central limit theorem,  $\int_{t'}^{t'+t_b} dt I_{on}(t)$  follows Gaussian statistics). Therefore the ratio  $\sqrt{\langle \delta I_{T_{photon}}^2 \rangle} / \langle I_{T_{photon}} \rangle$  scales as  $t_b^{-0.5}$ . Using this scaling and Eqs. (1) and (2), the RSD for conventional dye molecules can be approximated as

$$\frac{\sqrt{\langle \delta I_{T_{photon}}^2 \rangle}}{\langle I_{T_{photon}} \rangle} \propto \frac{1}{\sqrt{N_T t_b}}. \quad (6)$$

Equation (6) also applies to the photon emission statistics for QDs prior to the steady state. The experiments described in Figs. 2(a)–2(c) show that the motional narrowing effect applies to QDs in the transient equilibrium states. These experiments further imply that the lower cutoff values are much smaller than the bin size used. A snapshot fluorescence image taken from blinking CdSe(ZnS) QDs with a bin size of  $0.2$  sec in the transient equilibrium state as shown in Fig. 2(a) is compared to a snapshot image with the same bin size in the steady state in Fig. 2(b) and the integrated image that was accumulated for  $2.2$  h where the starting point was given at  $t=0$  in Fig. 2(c) (within this time, the time trace reaches its steady state). The relative density of emissive QDs shown in Fig. 2(c) is matched with that in Fig. 2(a), indicating that nearly every QD has emitted photons during a single bin in the transient equilibrium state. This is a clear signature that the motional narrowing effect<sup>26,27</sup> governs the

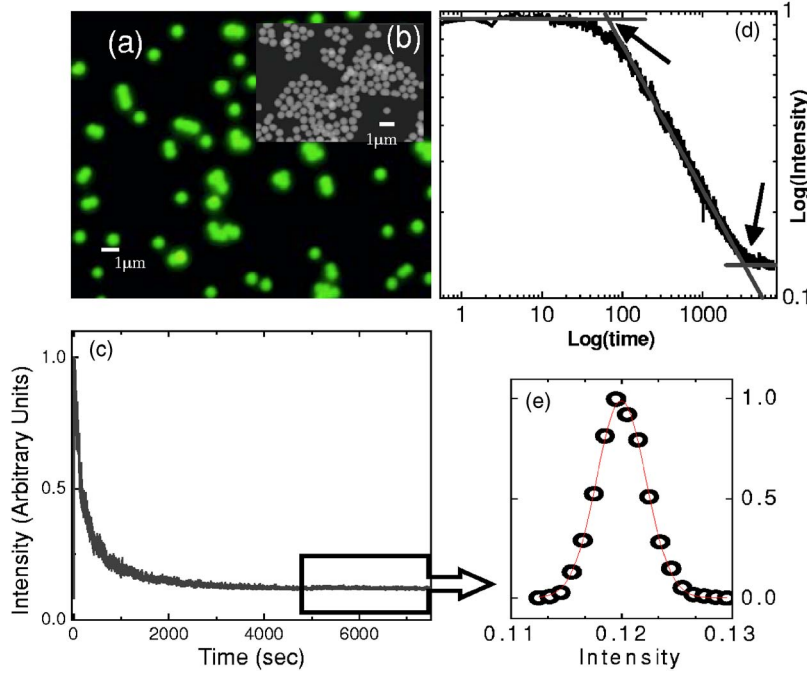


FIG. 3. (Color online) (a) A fluorescence image of QD-embedded core-shell silica microspheres with an average diameter of 447 nm. The scale bar corresponds to 1  $\mu\text{m}$ . (b) TEM image of these microspheres. (c) A fluorescence intensity time trace of a single microsphere where the boxed region indicates the steady-state regime. (d) Log-log plot of the trace in (c) where the two arrows indicate the on-time and off-time upper cutoffs. (e) The fluorescence intensity ( $I$ ) distribution of the boxed region in (c). The y axis corresponds to the probability density, normalized to 1. The average value  $\langle I \rangle$  is 0.12 and its width is 0.0044.

transient equilibrium state. This result also further implies that the lower cutoffs are much smaller than the binsize of 0.2 sec within which numerous rapid blinking events must take place.

Now, we demonstrate the use of Eq. (5) to estimate the number of QDs incorporated in the shell of a silica microsphere,<sup>24</sup> and this value is compared with that obtained from a conventional absorption method. Figure 3(a) shows a fluorescence microscope image of the microspheres dropcast from ethanol onto a glass substrate. The microspheres were synthesized according to a previously described procedure. The transmission electron microscope (TEM) image of these microspheres, shown in Fig. 3(b), demonstrates their narrow size distribution. Figures 3(c) and 3(d) show a fluorescence time trace for a single microsphere on a linear and log-log plot, respectively. The process to estimate the number of QDs from their ensemble time trace using Eq. (5) is described as follows. Equation (5) suggests that  $f_{on}^{ss} (\equiv p_{on})$  is the only parameter that is required to estimate the number of QDs,  $N_T$ . Acquiring an absolute value for  $f_{on}^{ss}$  involves these sequential steps: obtaining the ratios  $t_{off}^{max}/t_{on}^{max}$  and  $f_{on}^{te}/f_{on}^{ss}$  from the log-log plot of a time trace, such as in Fig. 3(d), and then estimating  $t_{off}^{min}/t_{on}^{min}$  using the two ratios  $t_{off}^{max}/t_{on}^{max}$  and  $f_{on}^{te}/f_{on}^{ss}$ , which ultimately yields absolute values for  $f_{on}^{te}$  and  $f_{on}^{ss}$ . Previous work demonstrated that  $f_{on}^{te}$  and  $f_{on}^{ss}$  can be estimated using only the two ratios  $t_{off}^{max}/t_{on}^{max}$  and  $f_{on}^{te}/f_{on}^{ss}$  if step function cutoffs are assumed and  $\mu_{on} = \mu_{off} = 0.5$  as shown in Eq. (7).<sup>2</sup> The analytical expressions for  $f_{on}^{te}$  and  $f_{on}^{ss}$  become complicated when  $\mu_{on} \neq \mu_{off}$  or if the cutoffs are smooth, although they can be easily calculated numerically. In Ref. 2, we assumed a step function cutoff at short times to estimate the values of  $f_{on}^{te}$  and  $f_{on}^{ss}$ . We also showed that different functional forms for the cutoffs do not significantly affect the absolute values of  $f_{on}^{te}$  and  $f_{on}^{ss}$ , or the value of  $f_{on}^{te}/f_{on}^{ss}$ . Choosing a step function for the short-time cutoffs simplifies the expressions for  $f_{on}^{te}$  and  $f_{on}^{ss}$  so that they are only functions of  $t_{off}^{min}/t_{on}^{min}$  and  $t_{off}^{max}/t_{on}^{max}$ , as shown in Eq. (7),

$$f_{on}^{te} = 1/[1 + (t_{off}^{min}/t_{on}^{min})^{0.5}],$$

$$f_{on}^{ss} = 1/[1 + (t_{off}^{min}/t_{on}^{min})^{0.5}(t_{off}^{max}/t_{on}^{max})^{0.5}]. \quad (7)$$

We therefore use Eq. (7) to estimate the number of QDs in a single microsphere of Fig. 3. First one needs to properly subtract the background intensity from the time trace. As indicated by the arrows in Fig. 3(d), the upper cutoff values  $t_{on}^{max}$  and  $t_{off}^{max}$  for QDs in the sphere are estimated to be 56 and 3620 sec, respectively. These values yield  $t_{off}^{max}/t_{on}^{max} = 64.6$ . Moreover, from the time trace, the ratio between the transient state intensity and the steady-state intensity,  $f_{on}^{te}/f_{on}^{ss}$ , is measured to be 6.59. With these two ratios and using Eq. (7), we find  $t_{off}^{min}/t_{on}^{min} = 14.8$ . With values for the two ratios  $t_{off}^{max}/t_{on}^{max}$  and  $t_{off}^{min}/t_{on}^{min}$ , Eq. (7) gives absolute values for  $f_{on}^{te}$  and  $f_{on}^{ss}$  as 0.25, and 0.046, respectively. Figure 3(e) shows a Gaussian distribution of fluorescence intensities obtained from a single microsphere in the steady-state regime as indicated by the boxed data of 3(c). From the Gaussian intensity distribution, the experimental RSD value is calculated to be 0.037.

With  $f_{on}^{ss} \equiv p_{on} = 0.046$  and the experimental RSD value as 0.037 for the fluorescence from a single microsphere at the steady state, we now estimate the total number of QDs in that microsphere to be  $1.5 \times 10^4 \pm 4.8 \times 10^2$  using Eq. (5). [The error bar is obtained by considering the uncertainties of the mean and the standard deviation values in Fig. 3(e)]. An absorption measurement yields a value of  $1.7 \times 10^4 \pm 0.2 \times 10^4$  QDs on average per microsphere as described in Refs. 23 and 28. Considering that the absorption measurement may contain QDs that are permanently dark, it can produce an overestimate for the number of emitting QDs in a sphere since fluorescence-based measurements only take into account those QDs that are emissive. The number of QDs in a single microsphere estimated by the method of this paper is, nevertheless, quite consistent with the number estimated from an absorption measurement on an ensemble of

microspheres.<sup>22,24</sup> Although our fluorescence based measurement does not count the QDs that are permanently dark, in applications of QDs that rely on their fluorescence, as well as in many fundamental questions about the dynamics of the fluorescence from QDs, it is the subpopulation that emits that is the interesting one. Therefore in many cases, a lack of information about the population of dark QDs is not necessarily a disadvantage. Overall, the method of the present work demonstrates a simple route for obtaining the number of emissive QDs incorporated in a microstructure. The long acquisition time may be considered a drawback of the method, and if an absorption measurement were indeed feasible, it would undoubtedly be the preferred method. However, an absorption measurement is often impossible when considering QDs within a microstructured device (for example, in a QD-based LED, or a microsphere incorporating QDs), where that device structure causes strong scattering, or if the device or the number of QDs is too small for a reliable absorption experiment.

### APPENDIX

Let  $I_{on}$  be an indicator function that yields 1 if a chromophore is on and 0 if off. Then the length of time  $t_{on}$  that the chromophores is on during a time period  $t_b$  is  $t_{on} = \int_{t'}^{t'+t_b} dt I_{on}(t)$ , where  $t'$  is an arbitrary starting point.

If the photon emission of chromophores that are on follows Poisson statistics, the probability that the chromophore emits  $m$  photons during  $t_b$  is shown in Eq. (A1)

$$P(m, t_b) \sim \frac{\left( \lambda \int_{t'}^{t'+t_b} dt I_{on}(t) \right)^m}{m!} e^{-\left( \lambda \int_{t'}^{t'+t_b} dt I_{on}(t) \right)}. \quad (\text{A1})$$

where  $\lambda$  is a Poisson parameter, specifically the rate of photon emission for the chromophore.

For an arbitrary blinking time sequence, the expectation values for  $m$  and  $m^2$  are

$$\langle m \rangle \equiv \lambda t_{on} = \lambda \int_{t'}^{t'+t_b} dt I_{on}(t),$$

$$\langle m^2 \rangle = \lambda^2 \left( \int_{t'}^{t'+t_b} dt I_{on}(t) \right)^2 + \lambda \int_{t'}^{t'+t_b} dt I_{on}(t). \quad (\text{A2})$$

Averaging these expressions over an entire blinking sequence results in  $\langle\langle m \rangle\rangle$  and  $\langle\langle m^2 \rangle\rangle$ , respectively. The variance for  $m$  then corresponds to

$$\begin{aligned} \langle\langle \delta^2 m \rangle\rangle &= \langle\langle m^2 \rangle\rangle - \langle\langle m \rangle\rangle^2 = \lambda^2 \left\langle \left( \int_{t'}^{t'+t_b} dt I_{on}(t) \right)^2 \right\rangle \\ &+ \lambda \left\langle \int_{t'}^{t'+t_b} dt I_{on}(t) \right\rangle - \lambda^2 \left\langle \int_{t'}^{t'+t_b} dt I_{on}(t) \right\rangle^2 \\ &= \lambda^2 \left\langle \delta^2 \int_{t'}^{t'+t_b} dt I_{on}(t) \right\rangle + \lambda \left\langle \int_{t'}^{t'+t_b} dt I_{on}(t) \right\rangle \end{aligned} \quad (\text{A3})$$

and

$$\langle\langle m \rangle\rangle = \lambda \left\langle \int_{t'}^{t'+t_b} dt I_{on}(t) \right\rangle.$$

Now the mean and variance for the total number of photons emitted from  $N_T$  chromophores are given as  $\langle I_{T_{photon}} \rangle = N_T \langle\langle m \rangle\rangle$  and  $\langle \delta^2 I_{T_{photon}} \rangle = N_T \langle\langle \delta^2 m \rangle\rangle$ , respectively, as shown in Eqs. (1) and (2) in the text.

<sup>1</sup>I. Chung and M. G. Bawendi, Phys. Rev. B **70**, 165304 (2004).

<sup>2</sup>I. Chung, J. B. Witkoskie, J. S. Cao, and M. G. Bawendi, Phys. Rev. E **73**, 011106 (2006).

<sup>3</sup>J. Schuster, F. Cichos, and C. V. Borczyskowski, Appl. Phys. Lett. **87**, 051915 (2005).

<sup>4</sup>M. Nirmal, B. O. Dabbousi, M. G. Bawendi, J. J. Macklin, J. K. Trautman, T. D. Harris, and L. E. Brus, Nature (London) **383**, 802 (1996).

<sup>5</sup>A. L. Efros and M. Rosen, Phys. Rev. Lett. **78**, 1110 (1997).

<sup>6</sup>U. Banin, M. Bruchez, A. P. Alivisatos, T. Ha, S. Weiss, and D. S. Chemla, J. Chem. Phys. **110**, 1195 (1999).

<sup>7</sup>T. D. Krauss and L. E. Brus, Phys. Rev. Lett. **83**, 4840 (1999).

<sup>8</sup>M. Kuno, D. P. Fromm, H. F. Hamann, A. Gallagher, and D. J. Nesbitt, J. Chem. Phys. **112**, 3117 (2000).

<sup>9</sup>K. T. Shimizu, R. G. Neuhauser, C. A. Leatherdale, S. A. Empedocles, W. K. Woo, and M. G. Bawendi, Phys. Rev. B **63**, 205316 (2001).

<sup>10</sup>Y. Jung, E. Barkai, and R. J. Silbey, Chem. Phys. **284**, 181 (2002).

<sup>11</sup>X. Brokmann, J. P. Hermier, G. Messin, P. Desbiolles, J. P. Bouchaud, and M. Dahan, Phys. Rev. Lett. **90**, 120601 (2003).

<sup>12</sup>M. Kuno, D. P. Fromm, S. T. Johnson, A. Gallagher, and D. J. Nesbitt, Phys. Rev. B **67**, 125304 (2003).

<sup>13</sup>R. Verberk and M. Orrit, J. Chem. Phys. **119**, 2214 (2003).

<sup>14</sup>E. Barkai and G. Margolin, Isr. J. Chem. **44**, 353 (2004).

<sup>15</sup>O. Flomenbom and J. Klafter, Phys. Rev. Lett. **95**, 098105 (2005).

<sup>16</sup>A. Issac, C. von Borczyskowski, and F. Cichos, Phys. Rev. B **71**, 161302(R) (2005).

<sup>17</sup>J. Tang and R. A. Marcus, J. Chem. Phys. **123**, 054704 (2005).

<sup>18</sup>R. Verberk, J. W. M. Chon, M. Gu, and M. Orrit, Physica E (Amsterdam) **26**, 19 (2005).

<sup>19</sup>K. T. Shimizu, W. K. Woo, B. R. Fisher, H. J. Eisler, and M. G. Bawendi, Phys. Rev. Lett. **89**, 117401 (2002).

<sup>20</sup>M. Pelton, D. G. Grier, and P. Guyot-Sionnest, Appl. Phys. Lett. **85**, 819 (2004).

<sup>21</sup>D. S. Novikov, M. Drndic, L. S. Levitov, M. A. Kastner, M. V. Jarosz, and M. G. Bawendi, Phys. Rev. B **72**, 075309 (2005).

- <sup>22</sup>C. A. Leatherdale, W. K. Woo, F. V. Mikulec, and M. G. Bawendi, *J. Phys. Chem. B* **106**, 7619 (2002).
- <sup>23</sup>Y. Ebenstein, E. Nahum, and U. Banin, *Nano Lett.* **2**, 945 (2002).
- <sup>24</sup>Y. Chan, J. P. Zimmer, M. Stroh, J. S. Steckel, R. K. Jain, and M. G. Bawendi, *Adv. Mater. (Weinheim, Ger.)* **16**, 2092 (2004).
- <sup>25</sup>B. R. Fisher, H. J. Eisler, N. E. Stott, and M. G. Bawendi, *J. Phys. Chem. B* **108**, 143 (2004).
- <sup>26</sup>P. W. Anderson, *J. Phys. Soc. Jpn.* **9**, 316 (1954).
- <sup>27</sup>R. Kubo, *J. Phys. Soc. Jpn.* **9**, 935 (1954).
- <sup>28</sup>To determine the number of QDs per microsphere, 5.2 mg of dried microspheres were dispersed in 2.2 mL ethanol and 0.3 mL toluene. The optical density of this clear, index-matched

solution was measured at 350 nm, permitting the calculation of the number of QDs present as  $9.82 \times 10^{14}$  [reference can be found in C. A. Leatherdale, W. K. Woo, F. V. Mikulec, and M. G. Bawendi, *J. Phys. Chem. B* **106**, 7619 (2002)]. A transmission electron microscope (TEM) image of the spheres was analyzed by ImageJ (<http://rsb.info.nih.gov/ij>) to determine the average sphere radius (223.5 nm) based on 100 spheres. This radius was used to calculate the volume of one sphere. The reported density of these spheres (Polysciences datasheet 635),  $1.96 \text{ g/cm}^3$ , was used to determine the mass of one sphere. The number of spheres could then be obtained as  $5.67 \times 10^{10}$ . This gives  $1.73 \times 10^4$  QDs per sphere.